

# GALACTOCEREBROSIDE-PHOSPHOLIPID INTERACTIONS IN BILAYER MEMBRANES

M. J. RUOCCO AND G. G. SHIPLEY

*Biophysics Institute, Departments of Medicine and Biochemistry, Boston University School of  
Medicine, Boston, Massachusetts 02118*

E. OLDFIELD

*School of Chemical Sciences, University of Illinois at Urbana-Champaign, Urbana, Illinois 61801*

**ABSTRACT** Differential scanning calorimetry (DSC) and x-ray diffraction have been used to study the interaction of hydrated *N*-palmitoylgalactosylsphingosine (NPGS) and dipalmitoylphosphatidylcholine (DPPC). For mixtures containing <23 mol % NPGS, complete miscibility of NPGS into hydrated DPPC bilayers is observed in both the bilayer gel and liquid-crystal phases. X-ray diffraction data demonstrate insignificant differences in the DPPC-bilayer gel-phase parameters on incorporation of up to 23 mol % NPGS. At >23 mol % NPGS, additional high-temperature transitions occur, indicating phase separation of cerebroside. For these cerebroside concentrations, at 20°C, x-ray diffraction shows two lamellar phases, hydrated DPPC-NPGS gel bilayers ( $d = 64 \text{ \AA}$ ) containing 23 mol % NPGS, and NPGS "crystal" bilayers ( $d = 55 \text{ \AA}$ ). On heating to temperatures >45°C, the mixed DPPC-NPGS bilayer phase undergoes chain melting, and on further increasing the temperature progressively more NPGS is incorporated into the liquid-crystal DPPC-NPGS bilayer phase. At temperatures >82°C (the transition temperature of hydrated NPGS), complete lipid miscibility is observed at all DPPC/NPGS molar ratios.

## INTRODUCTION

Galactocerebroside is a lipid component that occurs in appreciable amounts in mammalian brain tissues, particularly myelin, and appears to have primarily a structural role in myelin formation and integrity (1, 2). Recently, the structure and properties of cerebroside have been studied by x-ray diffraction (3–7) and calorimetric methods (7–11). X-ray diffraction studies of synthetic cerebroside have been performed by Pascher and colleagues (4, 12). The detailed understanding of the structure of cerebroside bilayers and the molecular interactions generated by the galactose and sphingosine moieties of cerebroside stem from single crystal studies of a hydroxylated cerebroside,  $\beta$ -D-galactosyl-*N*-(2-D-hydroxyoctadecanoyl)-D-dihydro-sphingosine ( $C_{18}$ -hydroxy-cer or  $C_{18}$ -phrenosine) (12). The cerebroside molecules are shown to pack in a bilayer arrangement. The polar region of the bilayer consists of galactosyl units aligned almost parallel to the bilayer interface. Numerous hydrogen bond acceptor and donor groups (>NH, —OH, >C=O) allow the formation of extensive lateral hydrogen bond systems between galactose and sphingosine residues in the planes of the galactosyl and amide moieties, respectively.

Dr. Ruocco's present address is the Francis Bitter National Magnet Laboratory, Massachusetts Institute of Technology, Cambridge, Massachusetts 02139.

In this laboratory, systematic structural and calorimetric studies of anhydrous and hydrated semisynthetic galactocerebroside have been performed (7). In particular, anhydrous and hydrated  $C_{16}$ -cerebroside (*N*-palmitoylgalactosylsphingosine, NPGS) show evidence of complex polymorphic behavior and interconversions between stable and metastable structural forms. Hydrated  $C_{16}$ -cerebroside undergoes a high-temperature (82°C), high-enthalpy (17.5 kcal/mol NPGS), bilayer crystal to liquid crystal transition, which is attributed to both a stable hydrocarbon chain packing and a lateral intermolecular hydrogen bonding network (7). The limited hydration/swelling characteristic of NPGS may be due to this extensive hydrogen-bonded interfacial region (13).

Although the phase behavior and structure of cerebroside are reasonably well characterized (3–7, 9–12), the interaction of cerebroside with phospholipids has not been extensively studied. Initial calorimetric studies of natural cerebroside-phospholipid mixtures were reported by Ladbrooke et al. (14) and Clowes et al. (8). More recently, the thermal behavior of mixtures of human spleen glucocerebroside and dipalmitoylphosphatidylcholine (DPPC) (15) and mixtures of bovine brain cerebroside and dimyristoylphosphatidylcholine (DMPC) have been reported (16). Correa-Freire et al. (15) suggest that the in-plane distribution of glucocerebroside molecules is affected by the physical state of the lipid bilayer and by the glucocerebroside/DPPC molar ratio. Vibrational Raman spectra of the

bovine brain kerosine fraction in mixtures with DMPC suggest that the phospholipid disrupts the cerebroside chain packing and alters the cerebroside head-group conformation (17). In contrast to these thermotropic and conformational studies, no structural studies of the interaction of galactocerebroside and phospholipid have been reported. In this paper, we present findings from an x-ray diffraction and calorimetric study of the phase behavior of mixed NPGS/DPPC bilayers. Although neither NPGS nor DPPC is a major constituent of myelin or other membranes, their chemical homogeneity does permit a detailed structural analysis of their mutual interactions. This approach should provide the framework in which more complex interactions between natural mixed chain cerebroside and phospholipids can be understood.

## MATERIALS AND METHODS

### Samples

*N*-palmitoylgalactosylsphingosine was synthesized from pig brain cerebroside according to methods described by Skarjune and Oldfield (18). It is estimated that NPGS contains ~5% of the dihydrosphingosine derivative. The purity was checked by thin layer chromatography (TLC). The NPGS gave a single spot in the solvent system, chloroform/methanol/water/acetic acid (65:25:4:1, vol/vol) and was used without further purification. Certain batches of NPGS containing fatty acid, sphingosine, and other impurities were purified by silicic acid column chromatography, and the final lipid product was recrystallized from chloroform/methanol (2:1, vol/vol). The purified lipid gave a single spot by TLC.

Commercial grade DPPC (Calbiochem-Behring Corp., American Hoechst Corp., La Jolla, CA) was purified by silicic acid chromatography and shown to be >99% pure by TLC using chloroform/methanol/water/acetic acid (65:25:4:1, vol/vol) as eluting solvent.

### Sample Preparation

Anhydrous samples of NPGS and DPPC were weighed to the desired molar ratio directly into a glass tube with a central constriction. The NPGS-DPPC mixtures were completely dissolved in chloroform/methanol (2:1, vol/vol), the solvent was evaporated under nitrogen at 30–35°C, and the sample was placed in a vacuum overnight. Tubes containing various molar ratios were hydrated with the appropriate amount of doubly distilled water by introduction through a microsyringe. Unless otherwise noted (see hydration study), hydrated samples contained 70% water by weight. Tubes were purged with nitrogen and immediately flame sealed. Equilibration of the hydrated lipid mixtures was achieved by repeated centrifugation through the central constriction for 1–10 min at  $T > T_m$  (NPGS) (i.e., 82°–90°C) followed by longer equilibration periods (1–2 h), at  $T > T_m$  (DPPC) (i.e., 50°–60°C). Equilibrated samples were monitored by TLC and used when determined to have insignificant amounts of impurities. In some instances lipid mixtures prepared directly into DSC pans were equilibrated by centrifuging the differential scanning calorimetry pans at appropriate temperatures. Consistent and reproducible behavior was obtained with both methods of equilibration.

Upon equilibration of the sample, the constricted tube was cooled to room temperature, opened, immediately mixed, and the well-mixed samples were taken for DSC and x-ray diffraction.

### Differential Scanning Calorimetry

Samples taken for calorimetry (1–15 mg) were hermetically sealed in stainless steel pans. Heating and cooling scans over the temperature range 20°–90°C were performed on a Perkin-Elmer (Norwalk, CT) DSC-2 scanning calorimeter using heating/cooling rates of 0.31°C/min to

5°C/min. Isothermal modes were also utilized. Transition temperatures were determined from the onset of the transition extrapolated to the baseline. Enthalpy measurements were determined from the area under the transition peak by comparison with those for a known standard (gallium). Baselines in the region of the transition were approximated by extrapolating the pretransition baseline to the posttransition baseline. Following the initial equilibration procedure (see Sample Preparation), various conditions were used to study the reproducible behavior of the cerebroside-phospholipid mixtures. The specific thermal pretreatment is described in the Results section. It should be noted that for some samples (see Fig. 1, *g* to *i*) difficulty was experienced in controlling the baseline curvature over the rather extensive temperature range, 0° to 95°C, used in these studies. However, it has been shown gravimetrically that no water loss from the DSC pan occurs as a result of this procedure.

### X-ray Diffraction

Hydrated samples were transferred to 1 mm ID capillaries (Charles Supper Co., Natick, MA). The capillary tubes were flame sealed and placed in a sample holder kept at constant temperature ( $\pm 0.5^\circ\text{C}$ ) by a circulating solvent/water bath. Nickel-filtered  $\text{CuK}_\alpha$  x radiation ( $\lambda = 1.5418 \text{ \AA}$ ) from an Elliot GX-6 rotating anode x-ray generator (Elliot Automation, Borehamwood, England) was focused by either a toroidal mirror optical camera or a double mirror optical camera. Diffraction patterns were recorded on Kodak No-Screen x-ray film (Eastman Kodak Co., Rochester, NY). Microdensitometry of x-ray photographs was carried out on a Joyce-Loebl model III-CS microdensitometer.

X-ray diffraction data were also recorded using a position-sensitive detector counter method. Nickel-filtered  $\text{CuK}_\alpha$  x radiation was produced from a microfocus x-ray generator (Jarrel-Ash Div., Fisher Scientific Co., Waltham, MA), line focused by a single mirror and collimated using the slit optical system of a Luzzati-Baro camera (E<sup>TS</sup> Beavdovin, Paris). X-ray diffraction data were recorded using a linear position sensitive detector (Tennelec, Inc., Oak Ridge, TN) and associated electronics (Tracor Northern, Middleton, WI).

## RESULTS

### Differential Scanning Calorimetry

The calorimetric thermograms of DPPC-NPGS lipid mixtures in 70% by weight  $\text{H}_2\text{O}$  are shown in Fig. 1. These calorimetric thermograms are representative first-heating scans following incubation of the mixtures in the calorimeter at 60°C, a temperature intermediate between the  $T_c$  of pure DPPC (41.6°C) and pure NPGS bilayers (82°C), for a predetermined period of time (~2 h) (see text below and compare Fig. 3). The samples were cooled to 23°C following the incubation period and immediately reheated.

Pure hydrated DPPC bilayers exhibit the characteristic pre- and main transitions at 35° and 41.6°C, respectively. The enthalpy of the hydrocarbon chain order-disorder transition is 8.7 kcal/mol DPPC (Fig. 1 *a*). In contrast, the chain melting transition of NPGS (Fig. 1 *j*) occurs at 82°C with a large enthalpy of 17.5 kcal/mol NPGS.

Addition of small quantities of cerebroside (<13 mol %) to hydrated DPPC bilayers results in a progressive increase in transition temperature ( $T_c$ ) of the main DPPC-rich gel to liquid crystal transition, from 41.6° to 44°C (Fig. 1 *a-c*, and Fig. 2 *a*). The temperature of the pretransition also increases a few degrees, from 35°C at 0 mol % NPGS to 37°C at 11.1 mol % NPGS. At NPGS concentrations >11

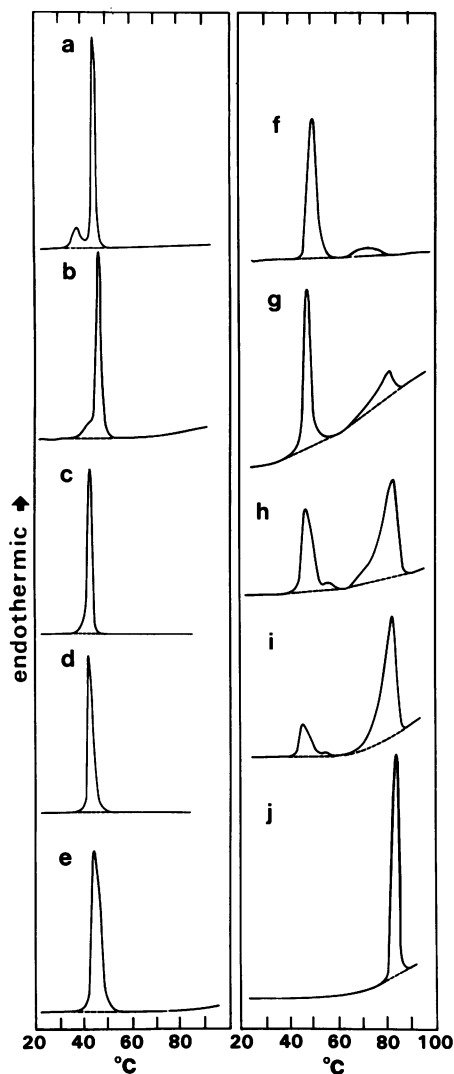


FIGURE 1 DSC of NPGS/DPPC lipid mixtures in 70% water by weight. Thermograms represent initial heating scans following incubation at 60°C for 2 h. Mixtures shown contain (a) 0, (b) 5.6, (c) 11.2, (d) 13.0, (e) 21.1, (f) 28.0, (g) 33.8, (h) 55.9, (i) 67.1, and (j) 100 mol % NPGS. Heating rate = 5°C/min.

mol % the pretransition is not observed (see ~13 mol % NPGS; Fig. 1 *d*). Further addition of NPGS to DPPC bilayers from 11 to ~21.1, mol % cerebroside results in a slight increase of  $T_c$  to 45°C for the DPPC-rich gel to liquid crystal transition (Figs. 1 *d* and 2 *a*). The  $T_c$  for this transition remains constant at ~45°C for mixtures containing greater concentrations of cerebroside (Fig. 1, *e* to *i*; Fig. 2 *a*, ■).

The enthalpy changes for the DPPC-rich gel to liquid crystal transition (Fig. 1, *a-d*) increase linearly from 8.7 kcal/mol DPPC for hydrated DPPC bilayers to 10.6 kcal/mol DPPC for DPPC bilayer containing 21.1 mol % cerebroside (Fig. 2 *b*). For cerebroside contents >21 mol %, the transition enthalpy for the DPPC-rich gel to liquid crystal transition levels off at  $\Delta H = 11.0$  kcal/mol DPPC in the 21–30 mol % NPGS compositional range, and then

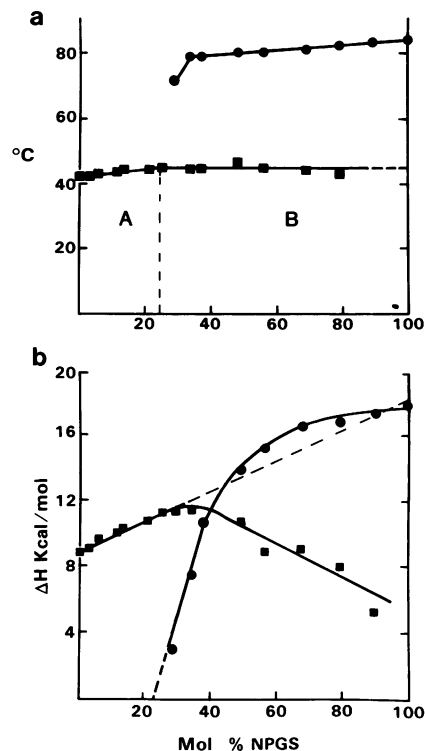


FIGURE 2 (a) Transition temperatures for the low- and high-temperature transitions shown in Fig. 1. ■,  $T_c$  of low temperature endotherm; ●,  $T_p$  (peak) of broad high-temperature endotherm. A and B denote compositional domains referred to in Results. (b) Enthalpy,  $\Delta H$  (kcal/mol) of NPGS/DPPC mixtures. ■, enthalpy of low temperature endotherm (see Fig. 1) in kcal/mol DPPC; ●, enthalpy of high-temperature transition (see Fig. 1) in kcal/mol NPGS.

decreases at higher cerebroside contents (see Fig. 2 *b* and discussion below).

At compositions >20 mol % NPGS, a second high-temperature transition occurs (Fig. 1 *f-i*). The DPPC-NPGS mixture containing 28 mol % NPGS exhibits a broad high-temperature transition at 70°C ( $T_{peak}$ ) with an enthalpy of 3.0 kcal/mol NPGS (Fig. 1 *f*). At 33.8 mol % NPGS, this broad asymmetric endotherm has increased to 78°C and has an enthalpy of 7.4 kcal/mol NPGS. Further increase of cerebroside content results in a slight increase in  $T_p$  of the second transition from 78° to 82°C (Fig. 1, *g-i*, and Fig. 2 *a*). In contrast, there is no significant increase in transition temperature of the low-temperature DPPC-rich gel to liquid crystal transition over this compositional range. The high-temperature transition becomes progressively dominant (Fig. 1, *f-i*) as additional cerebroside is added. The enthalpy of this transition increases from 3.0 kcal/mol NPGS at 28 mol % NPGS to 17.2 kcal/mol NPGS at 88.9 mol % NPGS (Fig. 2 *b*). The latter enthalpy value is similar to that of the order-disorder transition of pure C<sub>16</sub>-cerebroside bilayers (7). Interestingly, the enthalpy of the low-temperature DPPC-rich gel to liquid crystal transition (Fig. 1, *h-i*, and Fig. 2 *b*) at cerebroside compositions >50 mol % NPGS decreases from ~11.0

kcal/mol DPPC to 5.2 kcal/mol DPPC at 89.5 mol % NPGS.

The enthalpy data in Fig. 2 *b* indicate that for cerebroside concentrations  $\leq 23$  mol % there is a linear increase of  $\Delta H$  with increasing cerebroside content for the low-temperature endotherm, which is indicative of two miscible lipid components. Beyond this concentration there is the appearance of an additional high-temperature transition.

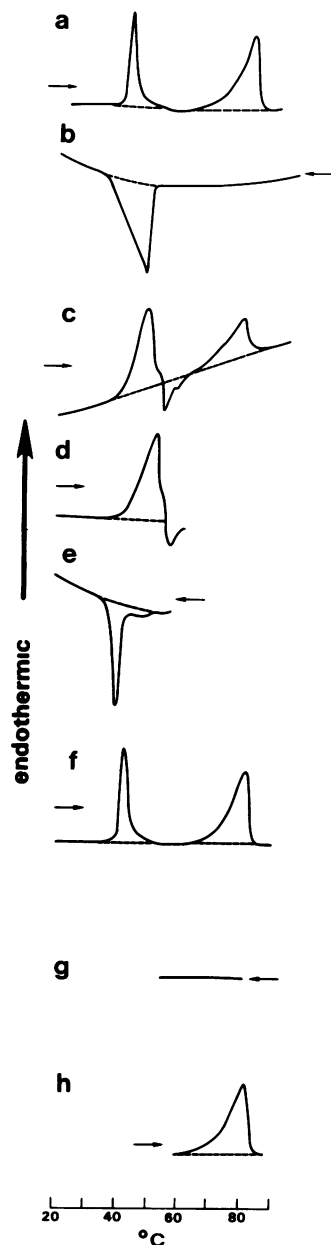


FIGURE 3 DSC of NPGS/DPPC (50.3:49.7 mol %) mixture. (a) Initial heating scan following incubation for 3 h at 60°C; (b) immediate cooling scan; (c) immediate reheating scan from 20° to 90°C; (d) heating scan to 60°C with an isothermal incubation at 60°C for ~3 h; (e) cooling scan from 60° to 20°C following incubation for ~3 h; (f) immediate reheating run following scan e; (g) immediate cooling scan to 60°C followed by isothermal incubation at 60°C for ~3 h; (h) heating scan from 60° to 90°C following incubation at 60°C. Heating/cooling rate = 5°C/min.

Analyzing the enthalpy of this high-temperature transition in terms of total cerebroside present in the mixture vs. the known  $\Delta H$  for the pure hydrated cerebroside crystal to liquid crystal transition allows a quantitation of the amount of cerebroside not participating in the cerebroside high-temperature transition. Both quantitation of these enthalpy data and extrapolation of the  $\Delta H$  data for the high temperature endotherm (see Fig. 2 *b*) indicate that  $23 \pm 3$  mol % NPGS does not cooperatively melt at the high temperature cerebroside crystal to liquid crystal transition. This amount of NPGS is incorporated into the DPPC-rich bilayers.

Based on these temperature and enthalpy data the temperature-composition diagram in Fig. 2 *a* can be divided into two compositional domains (A and B). These compositional domains have been further characterized by calorimetry and x-ray diffraction (see below).

In those binary mixtures containing  $\leq 23$  mol % cerebroside, (i.e., in mixtures where the cerebroside and phospholipid are miscible; domain A), the thermal behavior shown in Fig. 1, *a-e*, is reproducible. In contrast, at higher contents of cerebroside, domain B, the thermal behavior recorded is dependent upon the thermal history of the binary mixture. Fig. 3 summarizes the thermal behavior of a 50.3 mol % NPGS mixture that is representative for samples having compositions in domain B. The thermogram shown in Fig. 3 *a* is the first heating scan (5°C/min) following incubation of the mixture at a temperature (60°C) intermediate between the melting temperatures of pure DPPC and pure NPGS dispersions for 3 h. The low-temperature transition occurs at 45°C with an enthalpy of 10.6 kcal/mol DPPC followed by a high-temperature transition at 80°C with an enthalpy of 14.0 kcal/mol NPGS. Cooling at 5°C/min to 20°C (Fig. 3 *b*) results in a single asymmetric exotherm having a sharp high-temperature onset at 50°C. Immediate reheating from 20° to 90°C (Fig. 3 *c*) results in a large low-temperature endotherm at ~45°C, followed by an asymmetric exotherm ( $T_p = 56^\circ\text{C}$ ). The exotherm is immediately followed by a high-temperature endotherm at 78°C. The enthalpy of the high-temperature transition is now

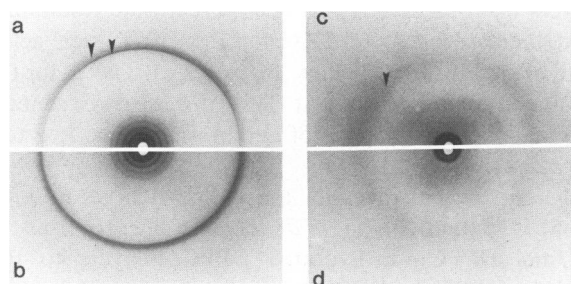


FIGURE 4 X-ray diffraction patterns of NPGS/DPPC mixtures (70% water by weight) containing (a) 0 mol % NPGS; (b) 21.1 mol % NPGS at 22°C; (c) 0 mol % NPGS; (d) 21.1 mol % NPGS at 60°C. Arrows correspond to wide-angle reflections noted in text.

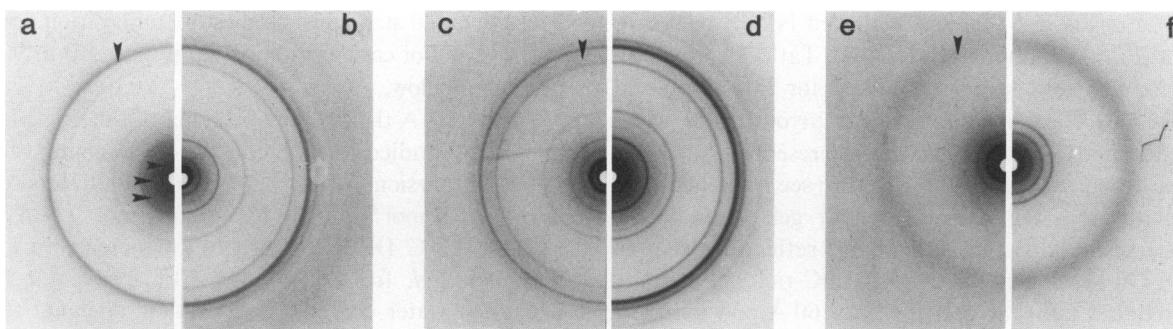


FIGURE 5 X-ray diffraction patterns of a NPGS/DPPC (50.3:49.7 mol %) mixture (70% water by weight); (a) NPGS/DPPC (50.3:49.7) mixture at 22°C, arrows indicate the low-angle lamellar Bragg spacings of the DPPC-rich gel and wide-angle reflections noted in text; (b) diffraction pattern of stable hydrated crystal form of NPGS (crystal E form) at 22°C; (c) NPGS/DPPC (50.3:49.7) mixture at 62°C, arrow indicates position of the  $\sim 1/4.5 \text{ \AA}^{-1}$  reflection from the disordered hydrocarbon chains of the melted DPPC-rich liquid-crystal phase; (d) hydrated stable form of NPGS (crystal E form) at 60°C; (e) NPGS/DPPC (50.3:49.7) mixture at 85°C, liquid-crystal form; (f) hydrated NPGS at 85°C, liquid-crystal form.

reduced to  $\sim 9$  kcal/mol NPGS. If the system is repeatedly heated and cooled between 20° and 90°C at 5°C/min, the behavior recorded in Fig. 3 *b* and *c* is reproduced. Alternatively, heating to 60°C and holding isothermally for 1–3 h (Fig. 3 *d*) results in the observation of a sharp exotherm at 40°C upon cooling to 20°C (Fig. 3 *e*). Immediate reheating from 20°C at 5°C/min yields the calorimetric behavior recorded initially after equilibration at 60°C (see Fig. 3, *a* and *f*); that is, the low-temperature endotherm at 45°C ( $\Delta H = 10.6$  kcal/mol DPPC) and the high-temperature endotherm at 80°C ( $\Delta H = 14.0$  kcal/mol NPGS) are again obtained. Similarly, cooling the melted system from 90° to 60°C (Fig. 3 *g*) and incubating the sample at 60°C for  $\sim 2$  h before reheating to 90°C results in the observation of the high-temperature endotherm at 80°C with only a slightly reduced enthalpy of 13.5 kcal/mol NPGS. This calorimetric behavior suggests that once both lipid components are melted at  $T \geq 82^\circ\text{C}$ , all melted cerebroside is miscible with DPPC in the liquid-crystal phase. The excess cerebroside does not immediately separate out of the mixed DPPC-NPGS bilayers at lower temperatures as the mixture is cooled, unless the system is allowed a sufficiently long equilibration period at an intermediate temperature ( $\sim 60^\circ\text{C}$ ).

### X-ray Diffraction

Structural studies of NPGS-DPPC binary mixtures containing 70%  $\text{H}_2\text{O}$  by weight are summarized in Figs. 4–7. The x-ray diffraction pattern for the hydrated DPPC gel phase at 22°C gives a set of lamellar spacings with a periodicity of 64 Å (Fig. 4 *a*). The sharp  $1/4.2 \text{ \AA}^{-1}$  and broad  $1/4.1 \text{ \AA}^{-1}$  reflections (arrows) indicate a tilted  $L_\beta'$  gel phase (see reference 19).

The mixture containing 21.1 mol % NPGS (representative of compositional domain A, see Fig. 2 *a*), gives a single set of lamellar reflections of periodicity 64 Å (Fig. 4 *b*). The positions and intensities of the low-angle reflections are relatively unchanged. In contrast, in the wide-angle

region the broad reflection appears to be less well resolved from the sharp reflection at  $\sim 1/4.1 \text{ \AA}^{-1}$  (Fig. 4 *b*).

At 60°C ( $T > T_m$  [DPPC]), both DPPC and DPPC bilayers containing 21.1 mol % cerebroside yield essentially identical diffraction patterns, characterized by a reduced lamellar periodicity,  $d$ , of 60 Å, and a diffuse wide-angle reflection at  $1/4.5 \text{ \AA}^{-1}$  (Fig. 4 *c* and *d*). These diffraction patterns are characteristic of a single liquid-crystal bilayer phase ( $L_\alpha$ , see reference 19).

For a sample containing 50.3 mol % NPGS (domain B, see Fig. 2 *a*), the diffraction pattern shown in Fig. 5 *a* is obtained at 22°C. This diffraction pattern yields two sets of lamellar reflections with periodicities of 64 and 54.5 Å. The arrowed reflections in Fig. 5 *a* correspond to the 64 Å periodicity of the gel phase found at lower NPGS compositions in domain A (see Fig. 4 *b*). The reflections indexing on the 54.5 Å periodicity are indicated by the corresponding x-ray diffraction pattern of hydrated NPGS bilayers at 22°C (Fig. 5 *b*, see correspondence of reflections in Fig. 5 *a*

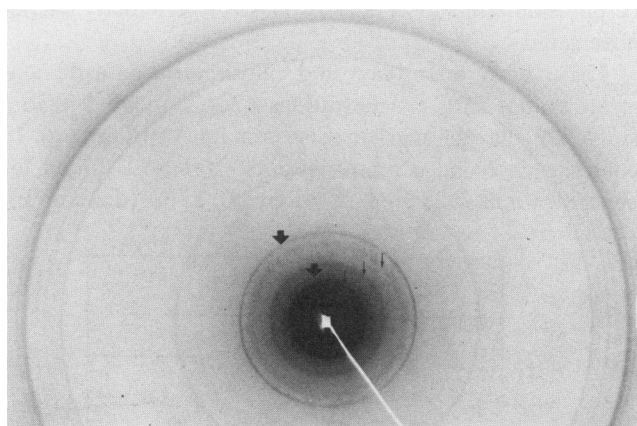


FIGURE 6 X-ray diffraction pattern of NPGS/DPPC (50.3:49.7 mol %) mixture (70% water by weight) at 22°C. Small arrows indicate low-angle reflections from the DPPC-rich lamellar gel phase, large arrows indicate the lamellar reflections from the NPGS crystal form.

with those in Fig. 5 *b* for pure hydrated NPGS bilayers). Using a Franks camera (Baird and Tatlock, London), better angular resolution is obtained for this sample at 22°C (Fig. 6). The low-angle (large arrows) and wide-angle reflections clearly indicate the presence of a stable hydrated cerebroside crystal (crystal E; see reference 7 for nomenclature); a DPPC-rich lamellar gel phase is also present (see additional low-angle reflections, small arrows). On heating to 62°C the DPPC-rich gel melts to give a reduced lamellar periodicity of 60 Å and a diffuse  $1/4.5 \text{ \AA}^{-1}$  reflection (arrow in Fig. 5 *c*). Note there are no significant dimensional changes in the remaining reflections from the cerebroside crystal phase. The diffraction pattern for pure, hydrated cerebroside at the corresponding temperature (60°C) is shown in Fig. 5 *d*. At 85°C, a temperature exceeding the second high-temperature transition (see, for example, Fig. 3), a single set of lamellar reflections of periodicity 54.5 Å, and a diffuse  $1/4.6 \text{ \AA}^{-1}$  reflection are recorded (Fig. 5 *e*). This diffraction pattern demonstrates that at this temperature there is only a single liquid-crystal lamellar phase. Note that once cerebroside melts into the preexisting melted DPPC-rich bilayers, the intensities of the low-angle reflections change. This indicates that a structural modification of the bilayer relative to melted DPPC and NPGS bilayers (Fig. 5 *f*) has occurred upon complete incorporation of cerebroside at 85°C. A diffraction pattern identical to that shown in Fig. 5 *a* is recorded upon slow cooling to 22°C (i.e., two lamellar periodicities are present,  $d = 64 \text{ \AA}$  and  $d = 54.5 \text{ \AA}$ ). The single phase DPPC-NPGS liquid crystal therefore undergoes phase separation to a DPPC-rich gel and stable cerebroside crystal (crystal E) as it is slowly cooled.

The bilayer periodicity,  $d$ , analyzed as a function of cerebroside concentration at 22°C is shown in Fig. 7. At low NPGS concentrations (i.e.,  $\leq 28 \text{ mol \%}$ ), diffraction patterns characteristic of the DPPC-rich gel phase (see Fig. 4 *a*) yielding a single lamellar periodicity of  $\sim 64 \text{ \AA}$  are recorded. At  $\geq 28 \text{ mol \%}$  NPGS, the presence of an excess cerebroside lamellar crystal E phase of periodicity 54.5 Å is detected.

These x-ray diffraction and calorimetric data demonstrate that at 22°C concentrations  $\leq 20\text{--}28 \text{ mol \%}$  NPGS a single lamellar gel phase exists (domain A in Fig. 2 *a*). In contrast, a second cerebroside crystal phase is found for concentrations  $\geq 28 \text{ mol \%}$  NPGS at 22°C (domain B).

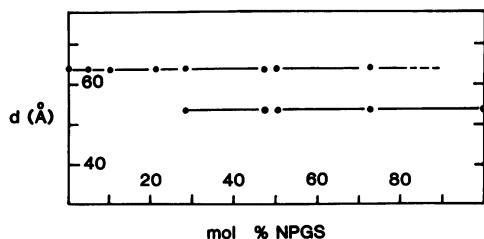


FIGURE 7 Lamellar periodicity,  $d$ , of NPGS/DPPC mixtures at various NPGS/DPPC compositions at 22°C.

More detailed structural studies of composition domain A at 22°C and of composition domains A and B at 90°C are presented below.

In domain A the swelling behavior of the single lamellar phase was studied as a function of water content for pure DPPC dispersions (Fig. 8 *a*) and DPPC dispersions containing 10.3 mol % (Fig. 8 *b*) and 21.1 mol % NPGS (Fig. 8 *c*). At 22°C DPPC undergoes an increase in lamellar periodicity,  $d$ , from 57.0 Å at 10% by weight  $\text{H}_2\text{O}$  to 64.0 Å at water contents greater than or equal to maximum hydration ( $\geq 30\%$  by weight  $\text{H}_2\text{O}$ ); see upper curve in Fig. 8 *a*. The corresponding swelling behavior at 22°C for DPPC dispersions containing 10.3 mol % and 21.1 mol % NPGS yield similar periodicity changes ranging from 56.5 Å (10.3 mol % NPGS) and 57.0 Å (21.1 mol % NPGS) at  $\sim 10\%$  by weight  $\text{H}_2\text{O}$  to 64.0 Å (10.3 mol % NPGS) and 64.2 Å (21.1 mol % NPGS) at maximum hydration ( $\sim 25\%$  by weight  $\text{H}_2\text{O}$ ); see upper curves in Fig. 8, *b* and *c*, respectively. These data demonstrate no significant difference in lamellar periodicity with swelling between pure, hydrated DPPC and DPPC dispersions containing between 10 and 21 mol % cerebroside.

At 60°C, hydrated DPPC containing 0 mol % NPGS forms a lamellar liquid crystal characterized by a disordered hydrocarbon chain packing. The diffraction patterns at various hydrations are characterized by a single set of lamellar spacings and a single diffuse wide-angle reflection

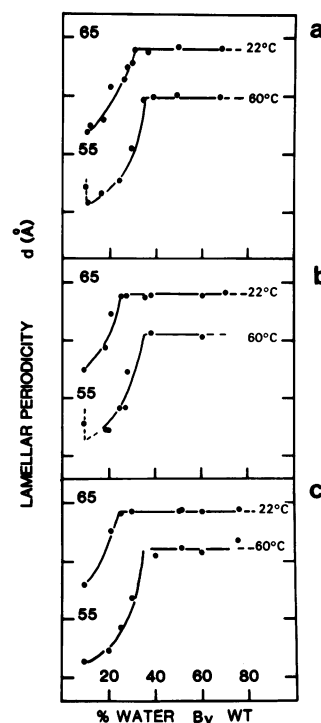


FIGURE 8 Lamellar periodicity,  $d$ , of NPGS/DPPC mixtures as a function of water concentration; (a) NPGS/DPPC, 0:100 mol % at 22°C (upper curve); at 60°C (lower curve); (b) NPGS/DPPC, 10.3:89.7 mol % at 22°C (upper curve); at 60°C (lower curve); (c) NPGS/DPPC, 21.1:78.9 mol % at 22°C (upper curve); at 60°C (lower curve).

at  $1/4.5 \text{ \AA}^{-1}$ . As expected, the maximum lamellar periodicity obtained at  $\sim 36\%$  water by weight is reduced to  $60 \text{ \AA}$  (see lower curve in Fig. 8 a). Incorporation of 10.3 to 21.1 mol % NPGS into DPPC lamellae at  $60^\circ\text{C}$  also results in a diffraction pattern having a single lamellar periodicity with a wide-angle reflection at  $1/4.5 \text{ \AA}^{-1}$  (for example, see Fig. 4). No significant changes in either the lamellar periodicity or the maximum hydration of DPPC bilayers containing these amounts (10.3 and 21.1 mol %) of NPGS are recorded (lower curves in Fig. 8 b and c).

From the swelling behavior of the DPPC and the single-phase DPPC-NPGS mixtures, the Fourier transform of the single bilayer can be sampled in such a way that the phase of each structure factor amplitude,  $F(s) [= \sqrt{I(s) \cdot h_{\text{corr}}^2}]$  can be determined (i.e.,  $\pi$  or 0). The plots of  $F(s)$  [ $s = 2 \sin\theta/\lambda$ ] for hydrated DPPC at  $22^\circ\text{C}$  containing 0, 10.3, and 21.1 mol % NPGS are given in Fig. 9 a, b, and c, respectively. Using the bilayer structure

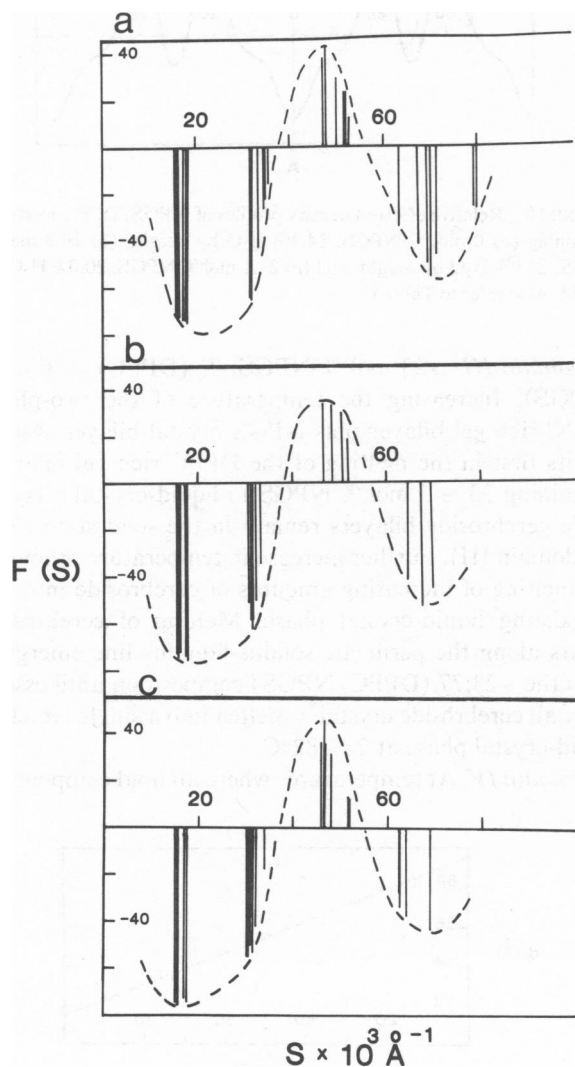


FIGURE 9 X-ray diffraction structure factor curves,  $F(s)$ , for hydrated NPGS/DPPC mixtures containing (a) 0, (b) 10.3, and (c) 21.1 mol % NPGS at  $22^\circ\text{C}$ .

factors  $F(s)$  shown in Fig. 9 to phase the lamellar reflections for the three bilayer systems allows the calculation of the relative electron density profiles,  $\rho(x)$ . The profiles of hydrated DPPC containing 0, 10.3, and 21.1 mol % NPGS at similar hydration levels at  $22^\circ\text{C}$  are shown in Fig. 10, a, b, and c, respectively. The profiles indicate a lamellar bilayer structure with two electron dense peaks corresponding to the galactose and/or phosphocholine head groups. Similar electron density profiles of hydrated DPPC in the  $L_\beta$  gel phase have been reported previously (19–22). The head group separation across the bilayer,  $d_{\text{polar-polar}}$ , remains constant at  $44 \text{ \AA}$ , even with incorporation of up to 21 mol % cerebroside (see Table I). At this resolution, the electron density profiles indicate no gross structural alterations of the cerebroside-containing bilayers relative to pure DPPC bilayers in either the low electron density methylene hydrocarbon and terminal methyl group regions or the high electron density head-group regions.

The structural behavior of DPPC-NPGS mixtures over the whole composition range was also studied at  $90^\circ\text{C}$ , ( $T > T_c$  [NPGS]), and the data are presented in Fig. 11. At  $90^\circ\text{C}$ , fully hydrated DPPC bilayers yield a lamellar periodicity of  $59.4 \text{ \AA}$  compared with a lamellar periodicity of  $51.5 \text{ \AA}$  for fully hydrated NPGS bilayers. Intermediate compositions of DPPC and NPGS mixtures yield a linear decrease of the lamellar periodicity from  $59.4 \text{ \AA}$  (DPPC bilayers) to  $51.5 \text{ \AA}$  (NPGS bilayers) as the amount of cerebroside in the mixture increases. This monotonic decrease in  $d$  is indicative of complete miscibility of the two components when the lipids are in the liquid crystalline state. Although four low-angle lamellar reflections were observed in the diffraction pattern for hydrated NPGS at  $90^\circ\text{C}$ , NPGS/DPPC mixtures exhibited only three lamellar orders at  $90^\circ\text{C}$ . This lack of diffraction data precluded a detailed structural analysis of the electron density profiles of DPPC and DPPC/NPGS liquid-crystal bilayers.

#### DISCUSSION

DSC of hydrated (70% by weight  $\text{H}_2\text{O}$ ) DPPC-NPGS mixtures (Fig. 1) over the  $20^\circ\text{--}90^\circ\text{C}$  range demonstrates that at low cerebroside concentrations ( $\leq 23$  mol % NPGS) there is a linear increase in  $T_c$  of the low-temperature endotherm from  $41.6^\circ$  to  $45^\circ\text{C}$  with a concomitant linear increase in the transition enthalpy from 8.7 to 10.6 kcal/mol DPPC (Fig. 2 b). The pretransition is completely

TABLE I  
STRUCTURAL PARAMETERS OF NPGS:DPPC  
BILAYERS

Temp $^\circ\text{C}$	mol % NPGS	% $\text{H}_2\text{O}$ by weight	$d$	$d_{\text{polar-polar}}$
22	0	24.3	62.7	44.0
22	10	21.0	62.3	44.0
22	21	20.0	62.6	44.0

absent upon the incorporation of ~13 mol % cerebroside (Fig. 1 *d*). At concentrations greater than ~23 mol % NPGS, a second high-temperature endotherm occurs (Fig. 1 *f*) at progressively higher temperatures (Fig. 2 *a*) and with larger enthalpies (Fig. 2 *b*) as greater amounts of cerebroside are added. The enthalpy data indicate a limiting value of  $23 \pm 3$  mol % cerebroside miscible in DPPC gel bilayers (Fig. 2 *b*).

Low-angle x-ray diffraction data (Fig. 7) indicate that at cerebroside concentrations approximately  $\geq 28$  mol %, a second lamellar periodicity of 54.5 Å is observed that is indicative of a second lamellar cerebroside phase. The inability to detect an excess cerebroside phase over the  $x_{\text{NPGS}} \leq 0.28$  range suggests that at the phase limit (i.e., in the calorimetrically determined range  $0.23 \geq x_{\text{NPGS}} < 0.28$ ) the excess cerebroside phase is insufficient to be detected by x-ray diffraction. The phase limits by calorimetry and x-ray diffraction are sufficiently close to define a phase limit of 20–28 mol % NPGS in gel DPPC bilayers.

The combined calorimetric and x-ray diffraction data allow the description of the phospholipid (DPPC)-cerebroside (NPGS) binary phase diagram in excess water (70% by weight). Fig. 12 shows that the NPGS-DPPC binary lipid phase diagram is of the peritectic type and defines four compositional domains, I–IV.

**Domain I:**  $\leq 23$  mol % NPGS;  $T < T_c$  (DPPC). A detailed study of  $d$  as a function of water indicates that at 22°C no significant dimensional changes occur with increasing amounts of cerebroside. Low-resolution electron-density profiles (Fig. 10 *a–c*) demonstrate that up to 21 mol % cerebroside can be incorporated into DPPC gel-phase bilayers without large structural alterations in the bilayer head group or hydrocarbon chain regions. Electron-density profiles at 22°C of DPPC containing 0, 10.3, and 21.1 mol % NPGS yield an invariant electron density profile and a constant bilayer thickness,  $d_{\text{polar-polar}} = 44$  Å. Higher resolution crystallographic analyses are required to determine better the effect of cerebroside incorporation on a molecular level.

The structural representation of this single gel phase is schematized in Fig. 12 (domain I). The cerebroside, as determined by x-ray diffraction and calorimetric methods, is totally miscible in the DPPC-rich bilayer gel phase.

**Domain II:**  $\geq 23$  mol % NPGS;  $T < T_c$  (DPPC). At 22°C, for concentrations of cerebroside greater than ~28 mol %, a second lamellar phase is detected by x-ray diffraction (Figs. 5 *a*, 6, and 7). This second phase has been shown by x-ray diffraction to be a separate cerebroside crystal E phase (Fig. 5 *b*) that is characterized by a number of wide-angle reflections indicative of a highly ordered cerebroside lamellar phase (7). From the estimated phase boundary, a DPPC-rich gel containing  $23 \pm 3$  mol % cerebroside ( $d \approx 64$  Å) (Fig. 5 *a*) is predicted to coexist with a second lamellar cerebroside crystal (crystal E) phase ( $d = 54.5$  Å) (see Fig. 12, domain II).

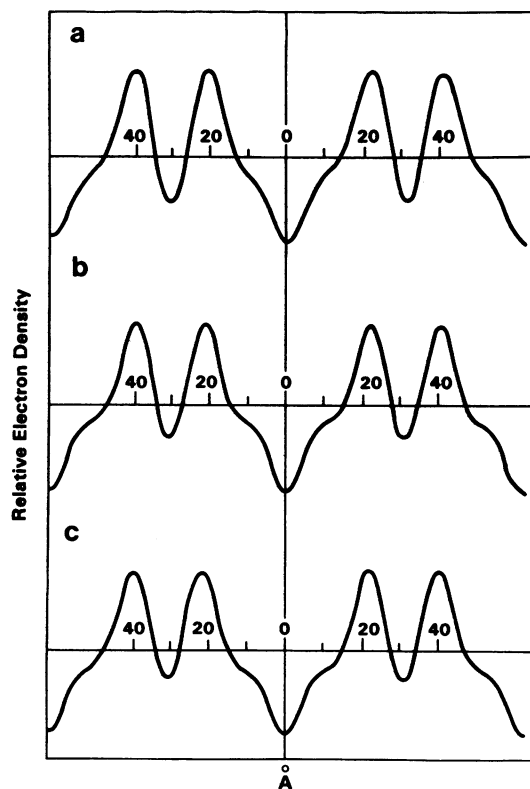


FIGURE 10 Relative electron density profiles of NPGS/DPPC mixtures containing (a) 0 mol % NPGS, 24.3% H<sub>2</sub>O by weight; (b) 10.3 mol % NPGS, 21.0% H<sub>2</sub>O by weight; and (c) 21.1 mol % NPGS, 20.0% H<sub>2</sub>O by weight. Also refer to Table I.

**Domain III:**  $> 23$  mol % NPGS;  $T_c$  (DPPC)  $< T < T_c$  (NPGS). Increasing the temperature of the two-phase DPPC-rich gel bilayer plus NPGS crystal-bilayer system results first in the melting of the DPPC-rich gel bilayers containing  $23 \pm 3$  mol % NPGS to liquid-crystal bilayers while cerebroside bilayers remain in the solid state (Fig. 12, domain III). Further increase in temperature promotes the melting of increasing amounts of cerebroside into the preexisting liquid-crystal phase. Melting of cerebroside occurs along the peritectic solidus-liquidus line emerging from the ~23:77 (DPPC/NPGS) composition until essentially all cerebroside crystal is melted into a single lamellar liquid-crystal phase at  $T > 82^\circ\text{C}$ .

**Domain IV.** At temperatures where all lipid components

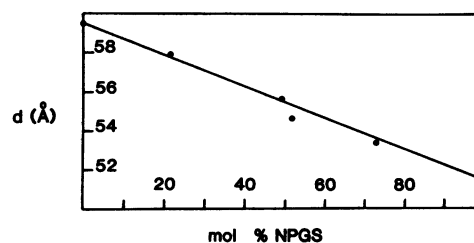


FIGURE 11 Lamellar periodicity,  $d$ , of NPGS/DPPC mixtures at  $90^\circ\text{C}$ .



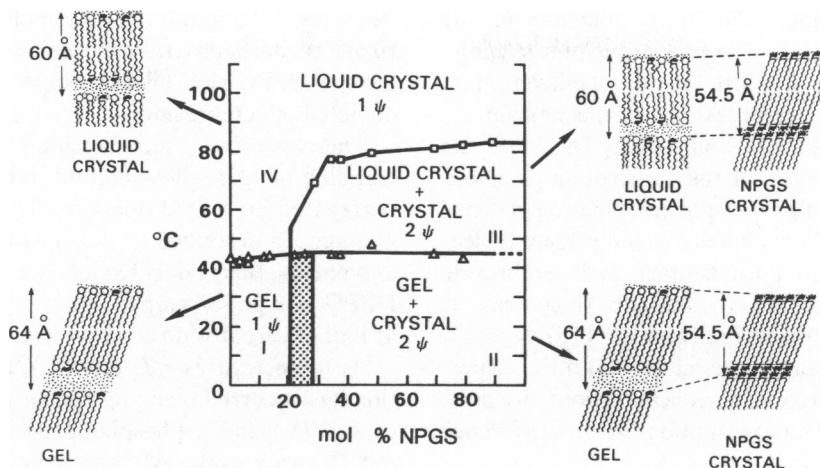


FIGURE 12 Temperature-composition phase diagram of NPGS/DPPC binary lipid system at 70% water by weight. Temperatures of DPPC-rich gel to liquid crystal transition ( $\Delta$ ) and NPGS crystal to NPGS liquid crystal transition ( $\square$ ) are indicated. *I-IV* correspond to compositional domains referred to in text. Schematic representations of the lamellar bilayer structures are presented and include Domain I, DPPC-rich gel, 1 lipid phase; Domain II: DPPC-rich gel ( $\sim 23$  mol % NPGS) and NPGS crystal, two lipid phases; Domain III, DPPC-rich liquid crystal ( $>23$  mol % NPGS) and NPGS crystal, two lipid phases; Domain IV, NPGS/DPPC liquid crystal, one lipid phase. (Note that the excess water phase is not considered in this phase diagram.) Phospholipid molecules are represented with circular head groups, cerebroside molecules are represented in black. On the basis of (a) the bilayer periodicity of anhydrous and hydrated NPGS (7), (b) model building studies (7), and (c) comparisons with the crystal structure of cerebroside (12), we have suggested earlier that the NPGS molecules adopt a tilted arrangement with respect to the bilayer normal in the NPGS crystal phase (7).

are in the liquid crystalline state,  $T > 82^\circ\text{C}$ , this region is characterized by complete miscibility of DPPC and NPGS at all compositions. The low-angle x-ray data at  $90^\circ\text{C}$  for a number of DPPC/NPGS compositions show a weight-averaged lamellar periodicity with variation of composition (Fig. 11). This is interpreted to be an indication of complete mixing of cerebroside and phospholipid at this temperature. For DPPC/NPGS compositions to the left of the liquidus line, again miscibility of the two lipids in a bilayer phase is observed at  $T > 42^\circ\text{--}45^\circ\text{C}$  (Fig. 12, domain IV).

The phase limit for cerebroside miscibility at temperatures just  $>T_c$  (DPPC) defined in this study is consistent with data reported in other cerebroside-phospholipid studies. Diphenylhexatriene fluorescence quenching studies using mixtures of bovine brain cerebroside with spin-labeled egg yolk lecithin indicate a maximum incorporation of  $\sim 20$  mol % cerebroside into liquid crystalline lecithin bilayers at  $23^\circ\text{C}$  (Curatolo and London, personal communication). Recently, Skarjune and Oldfield have reported a maximum solubility of 17% by weight ( $\sim 18$  mol %)  $C_{16}$ -glucocerebroside in liquid-crystal DMPC, DPPC, and DPPE bilayers at temperatures just above the phase transition temperature of the phospholipid component (23).

The defined phase behavior as summarized above and represented in Fig. 12 is given a molecular interpretation that is presented in Fig. 13 *A* and *B*. At concentrations of cerebroside  $>23$  mol %, a single bilayer phase exists in which cerebroside molecules (shown in black) mix into the DPPC-rich bilayer gel phase (Fig. 13 *A*). This gel phase melts to a disordered liquid crystal with no change in

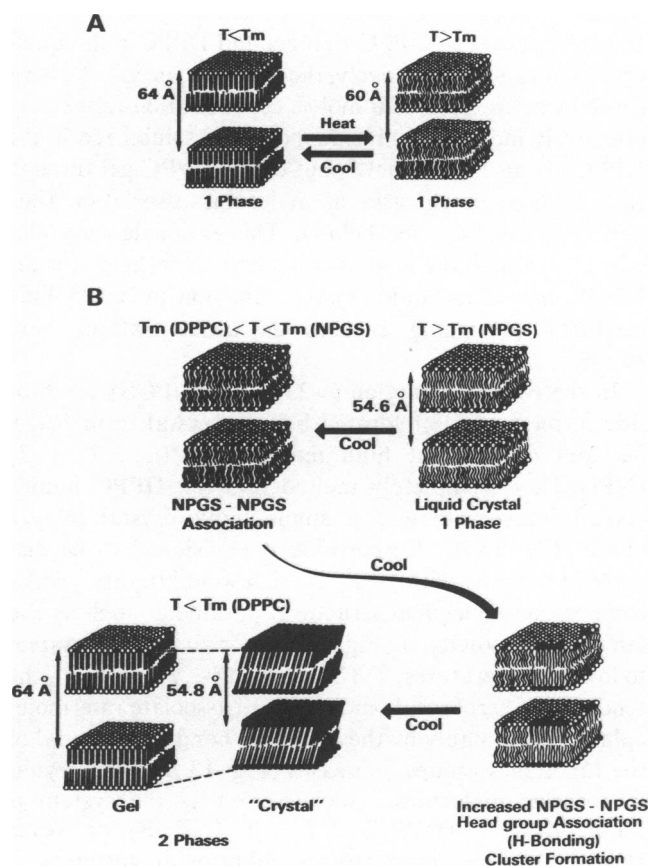


FIGURE 13 Representative molecular interpretation of structural behavior of NPGS/DPPC bilayers containing (A)  $<23$  mol % NPGS; (B) 50 mol % NPGS; black molecules represent cerebroside lipid molecules.

miscibility of cerebroside. The linear increase in the enthalpy for the gel to liquid crystal transition suggests that additional stability is imparted to the gel bilayer phase by the presence of the cerebroside. The mechanism for additional membrane stability would likely be due to the hydrogen-bonding capability of the cerebroside galactose and/or sphingosine moieties. The potential hydrogen donor and acceptor groups of these moieties would present molecular sites through which phospholipids and cerebroside molecules could intermolecularly associate. In contrast, it should be noted that Correa-Freire et al. (15) report a decrease in  $\Delta H$  for human glucocerebroside-DPPC dispersions with increasing cerebroside concentrations. At present, we have no convincing explanation for this difference in behavior.

For cerebroside-rich mixtures, the behavior is more complex. As shown in Fig. 2 *b* the enthalpy of the DPPC-rich gel to liquid crystal transition reaches a maximum of 11 kcal/mol DPPC at ~25–50 mol % NPGS. At greater concentrations of NPGS the enthalpy of this transition steadily decreases to ~5 kcal/mol DPPC at 90 mol % cerebroside. Although this behavior is not expected, partial explanation may be due to a large interfacial effect in the two phase regions (domains II and III) as the cerebroside domains effectively disorder the DPPC-rich phase thereby reducing cooperativity and/or the enthalpy necessary to transform between DPPC-rich gel and DPPC-rich liquid-crystal phases. Alternatively, the large proportion of excess cerebroside in the 50–90 mol % concentration range may effectively induce cerebroside molecules solubilized in the DPPC gel at  $23 \pm 3$  mol % out of the DPPC gel through the proposed mechanism of molecular association (i.e., hydrogen bonding, see below). This rationale may also partially explain the nonlinear increase in enthalpy for the NPGS crystal to liquid-crystal transition in binary-lipid mixtures containing cerebroside concentrations >50 mol %.

In the two-phase region (>23 mol % NPGS) cerebroside forms a stable hydrated bilayer crystal form (Figs. 5 *a* and 6) that, at high temperature (i.e.,  $T > T_c$  [NPGS]), is completely melted into the DPPC liquid-crystal bilayers to give a single liquid-crystal bilayer phase (Fig. 13 *B*). Cerebroside is envisioned to be dispersed randomly with DPPC, which would in turn yield a composition-dependent structural parameter such as the lamellar periodicity,  $d$  (Fig. 11). Upon cooling the system to lower temperatures,  $T_c$  (DPPC) <  $T < T_c$  (NPGS), the tendency of cerebroside molecules to associate intermolecularly, presumably by the hydrogen bonding potential of the functional groups, increases (Fig. 13 *B*). As a result, cerebroside molecules associate, and as the system is incubated at  $T_c$  (DPPC) <  $T < T_c$  (NPGS), or cooled slowly to lower temperatures, additional clustering is promoted. Finally, the cerebroside clusters fuse to form laterally (and eventually three-dimensionally) segregated

domains. Concomitantly, the melted DPPC-rich bilayer phase becomes progressively depleted of cerebroside. melted DPPC-rich bilayer phase becomes progressively depleted of cerebroside.

The clustering of cerebroside may also induce partial trapping of some phospholipid molecules in the laterally segregated glycolipid domains. This, in addition to those phenomena described above, may account in part for the anomalous thermal behavior (i.e., reduced  $\Delta H$ ) of the DPPC-rich gel-bilayer to liquid-crystal bilayer transition at higher cerebroside concentrations.

At temperatures <  $T_c$  (DPPC), ultimate phase separation has occurred, yielding both a stable hydrated NPGS crystal (E) and a phospholipid-rich gel containing ~23 mol % cerebroside. At rapid cooling rates ( $\geq 5^\circ\text{C}/\text{min}$ ), greater amounts of cerebroside, in excess of the miscibility limit, appear to remain in the DPPC gel. This condition is metastable; an equilibrated system is achieved by heating the cerebroside-supersaturated gel to ~60°C (i.e.,  $T_c$  [DPPC] <  $T < T_c$  [NPGS]) and incubating for a prolonged period (see Fig. 3). This results in the separation of an excess cerebroside phase.

This thermal and structural study of  $C_{16}$ -cerebroside indicates that the strong specific intermolecular interaction between cerebroside molecules accounts for the low miscibility of cerebroside in phosphatidylcholine gel phase bilayers. The phase behavior of the DPPC-NPGS model system may be of importance in predicting the behavior of cerebroside-containing membranes including myelin, spleen, and liver cellular membranes. Although the presence of other lipid components such as cholesterol, as well as the fatty acyl heterogeneity of cerebroside, may alter the solubility of cerebroside in these membranes (13, 16), a limiting concentration does exist where phase separation of cerebroside occurs. Evidence for this behavior is found in Gaucher's disease where tissue deposits of "insoluble" glucocerebroside-rich lamellar aggregates are found (24). In addition, in long-term organotypic cultures of central and peripheral nervous tissue, inclusions of galactocerebroside (25) similar to those described in Krabbe's globoid leucodystrophy are observed (26).

We wish to thank Drs. D. Atkinson and D. M. Small for valuable discussions and to acknowledge the assistance of Ms. Anne Gibbons in the preparation of this manuscript.

This work was supported by National Institutes of Health research grants HL-26335 and HL-07291.

Received for publication 4 January 1983.

## REFERENCES

1. Rumsby, M. G. 1978. Organization and structure in central nerve myelin. *Biochem. Soc. Trans.* 6:448–462.
2. Bologna-Sandru, L., B. Zalc, N. Herschkowitz, and N. Baumann. 1981. Oligodendrocytes of jimpy mouse express galactosylceram-

- ide: an immunofluorescence study on brain sections and dissociated brain cell cultures. *Brain Res.* 225:425–430.
3. Reiss-Husson, F. 1967. Structure des phases liquide-cristallines de differents phospholipides, monoglycerides, sphingolipides, anhydres ou en presence d'eau. *J. Mol. Biol.* 25:363–382.
  4. Abrahamsson, S., I. Pascher, K. Larsson, and K.-A. Karlsson. 1972. Molecular arrangements in glycolipids. *Chem. Phys. Lipids.* 8:152–179.
  5. Fernandez-Bermudez, S., J. Loboda-Cackovic, H. Cackovic, and R. Hosemann. 1977. Structure of cerebroside. I. Phrenosine at 23°C and 66°C. *Z. Naturforsch. Teil C.* 32:362–374.
  6. Hosemann, R., J. Loboda-Cackovic, and H. Cackovic. 1979. Structure of cerebroside. II. Small angle x-ray diffraction study of cerasine. *Z. Naturforsch. Teil C.* 34:1121–1124.
  7. Ruocco, M. J., D. Atkinson, D. M. Small, R. P. Skarjune, E. Oldfield, and G. G. Shipley. 1981. X-ray diffraction and calorimetric study of anhydrous and hydrated *N*-palmitoylgalactosylsphingosine (cerebroside). *Biochemistry.* 20:5957–5966.
  8. Clowes, A. W., R. J. Cherry, and D. Chapman. 1971. Physical properties of lecithin-cerebroside bilayers. *Biochim. Biophys. Acta.* 249:301–317.
  9. Bunow, M. R. 1979. Two gel states of cerebroside: calorimetric and Raman spectroscopic evidence. *Biochim. Biophys. Acta.* 574:542–546.
  10. Freire, E., D. Bach, M. Correa-Freire, I. Miller, and Y. Barenholz. 1980. Calorimetric investigation of the complex phase behavior of glucocerebroside dispersions. *Biochemistry.* 19:3662–3665.
  11. Curatolo, W. 1982. Thermal behavior of fractionated and unfractionated bovine brain cerebroside. *Biochemistry.* 21:1761–1764.
  12. Pascher, I., and S. Sundell. 1977. Molecular arrangements in sphingolipids. The crystal structure of cerebroside. *Chem. Phys. Lipids.* 20:175–191.
  13. Ruocco, M. J. 1983. Molecular interaction of cerebroside with phospholipid and cholesterol. Ph.D. Dissertation. Boston University.
  14. Ladbrooke, B. D., T. J. Jenkinson, V. B. Kamat, and D. Chapman. 1968. Physical studies of myelin. I. Thermal analysis. *Biochim. Biophys. Acta.* 164:101–109.
  15. Correa-Freire, M. C., E. Freire, Y. Barenholz, R. Biltonen, and T. E. Thompson. 1979. Thermotropic behavior of glucocerebroside-dipalmitoylphosphatidylcholine multilamellar liposomes. *Biochemistry.* 18:442–445.
  16. Linington, C., and M. G. Rumsby. 1981. Galactosyl ceramides of the myelin sheath: thermal studies. *Neurochem. Int.* 3:211–218.
  17. Bunow, M. R., and I. W. Levin. 1981. Molecular conformations of cerebroside in bilayers determined by Raman spectroscopy. *Biophys. J.* 32:1007–1021.
  18. Skarjune, R., and E. Oldfield. 1979. Physical studies of cell surface and cell membrane structure. Deuterium nuclear magnetic resonance investigation of deuterium-labelled *N*-hexadecanoylgalactosylceramide (cerebroside). *Biochim. Biophys. Acta.* 556:208–218.
  19. Tardieu, A., V. Luzzati, and F. C. Reman. 1973. Structure and polymorphism of the hydrocarbon chains of lipids: a study of lecithin-water phases. *J. Mol. Biol.* 75:711–733.
  20. Levine, Y. K., A. I. Bailey, and M. H. F. Wilkins. 1968. Multilayers of phospholipid bimolecular leaflets. *Nature (Lond.).* 220:577–578.
  21. Inoko, Y., and T. Mitsui. 1978. Structural parameters of dipalmitoyl phosphatidylcholine lamellar phases and bilayer phase transitions. *J. Phys. Soc. Japan* 44:1918–1924.
  22. McIntosh, T. J. 1978. The effect of cholesterol on the structure of phosphatidylcholine bilayers. *Biochim. Biophys. Acta.* 513:43–58.
  23. Skarjune, R., and E. Oldfield. 1982. Physical studies of cell surface and cell membrane structure. Deuterium nuclear magnetic resonance studies of *N*-palmitoylglucosylceramide (cerebroside) head-group structure. *Biochemistry.* 13:3154–3160.
  24. Lee, R. E., C. R. Worthington, and R. H. Glew. 1973. The bilayer nature of deposits occurring in Gaucher's disease. *Arch. Biochem. Biophys.* 159:259–266.
  25. Stern, J., A. B. Novikoff, and R. D. Terry. 1972. The induction of sulfatide, ganglioside and cerebroside storage in organized nervous system cultures. *Adv. Exp. Med. Biol.* 19:651–660.
  26. Suzuki, K., and Y. Suzuki. 1978. In *The Metabolic Basis of Inherited Disease*. J. B. Stanbury, J. B. Wyngaarden, and D. S. Fredrickson, editors. McGraw-Hill, Inc., New York, 747–769.